

21 **Abstract**

22 During sexual transmission, the large genetic diversity of HIV-1 within an individual is
23 frequently reduced to one founder variant that initiates infection. Understanding the drivers of
24 this bottleneck is crucial to develop effective infection control strategies. Little is known about
25 the importance of the source partner during this bottleneck. To test the hypothesis that the
26 source partner affects the number of HIV founder variants, we developed a phylodynamic model
27 calibrated using genetic and epidemiological data on all existing transmission pairs for whom the
28 direction of transmission and the infection stage of the source partner are known. Our results
29 suggest that acquiring infection from someone in the acute (early) stage of infection increases the
30 risk of multiple founder variant transmission when compared with someone in the chronic (later)
31 stage of infection. This study provides the first direct test of source partner characteristics to
32 explain the low frequency of multiple founder strain infections.

33

34

35 **Main Text**

36 Sexual transmission of HIV-1 results in a viral diversity bottleneck due to physiological barriers
37 as well as viral or cellular constraints that prevent most genetic variants within the source partner
38 from establishing onward infection (1–3). Indeed, this diversity bottleneck results in around three
39 quarters of new infections being founded by a single genetic variant (4–9). The extent of genetic
40 diversity transmitted to a new partner is a crucial determinant in understanding the efficacy of
41 putative vaccines and may shed light on the transmission of drug resistance to treatment naive
42 individuals.

43

44 The factors leading to the diversity bottleneck during sexual transmission can be broadly
45 categorized as those determined by the source partner—such as viral load and viral diversity
46 available for transmission (10), those determined by the recipient partner—such as target cell type
47 and availability in the genital or rectal mucosa (e.g. (3, 11, 12)), and those connected with viral
48 characteristics—such as glycosylation profiles and cell tropism (reviewed in (13)). While the
49 impact of the recipient partner and the characteristics of transmitted founder variants have been
50 widely discussed, little is known about how the source partner affects the viral diversity bottleneck.
51 Modelling work suggests that infection stage of the source partner at the point of onward
52 transmission may be a key driver in determining the number of transmitted variants (14). However,
53 there is currently no empirical evidence to suggest how the infection stage of the source partner
54 influences the viral diversity bottleneck. This gap has arisen because analyses are routinely
55 conducted on individuals without information on the partner from whom they acquired infection.
56 Phylogenetic analyses now offer a possible solution to this impasse.

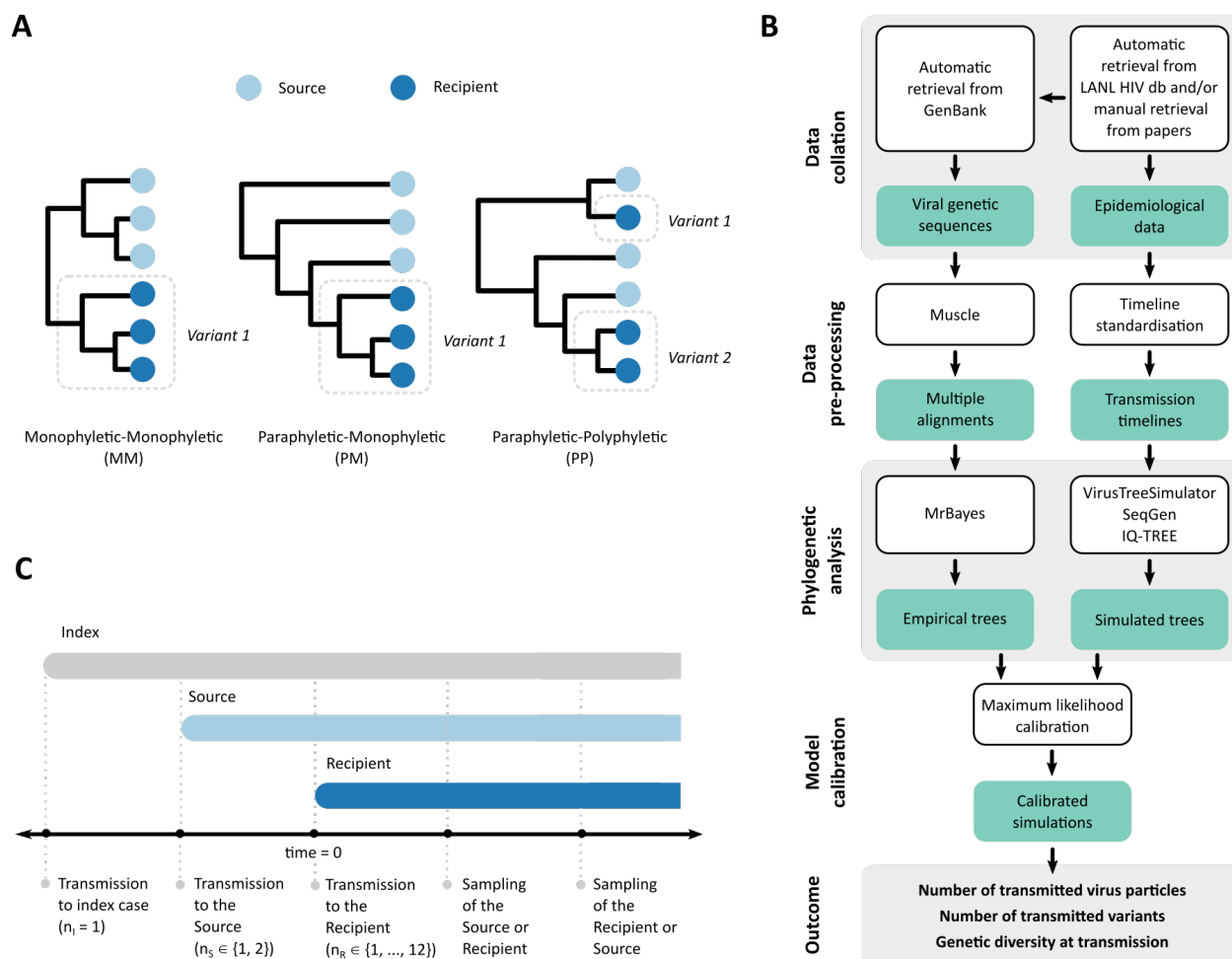
57

58 Phylogenetic trees are representations of the ancestral relationships of organisms with the tips of
59 the tree representing those that are sampled, the internal nodes representing their inferred
60 common ancestors, and the branches as the evolutionary pathways between these actual and
61 inferred individuals. When phylogenetic trees are constructed using sequence data from both
62 partners in an HIV transmission pair, the relationship between the evolutionary histories of both
63 sets of viral samples may reflect epidemiological relationships between the two individuals (15-
64 17). Previous modelling studies suggest that the evolutionary histories of the viral populations in
65 both partners can provide important information, such as the direction of transmission (15) and
66 the number of transmitted founder variants (18). For this, each putative transmission pair can be
67 classified into one of three ‘topologies’ that defines the evolutionary relationship between the
68 viral populations of the two partners: monophyletic-monophyletic (*MM*, where the sequences
69 from each partner form separate groups), paraphyletic-monophyletic (*PM*, where the sequences
70 from one partner are embedded in the sequences from the second partner), or a combination of
71 paraphyletic and polyphyletic (*PP*, where sequences from both partners are interspersed) (**Fig.**
72 **1A**). The number of monophyletic clusters in a *PM* (one) or *PP* (more than one) tree can be
73 interpreted as the minimum number of transmitted founder variants. In practice, however, many
74 factors may influence epidemiological interpretations from phylogenetic trees such as sampling
75 times, sampling density of the viral populations and phylogenetic signal (19, 20).

76

77 Here we present a data-driven phylodynamic approach to overcome these empirical and
78 methodological issues to evaluate the impact of the source partner’s infection stage and route of
79 exposure on the HIV diversity bottleneck (**Fig. 1B, C**). We first retrieved all available genetic
80 and epidemiological information from published HIV sexual transmission pairs where the

81 direction of transmission is known, and kept for further analysis those pairs for whom
 82 transmission could be classified as having occurred in the source partner's acute stage (≤ 90 days
 83 after his/her infection) or chronic stage (later than 90 days after his/her infection). After further
 84 stratifying pairs into heterosexual (HET) and men-who-have-sex-with-men (MSM) risk groups,
 85 we found a significant difference in the timing of transmission between the two risk groups.
 86 Specifically, 10 of 36 MSM pairs were the result of acute stage transmission compared with 1 of
 87 76 of HET pairs (**Fig. 2**).



88

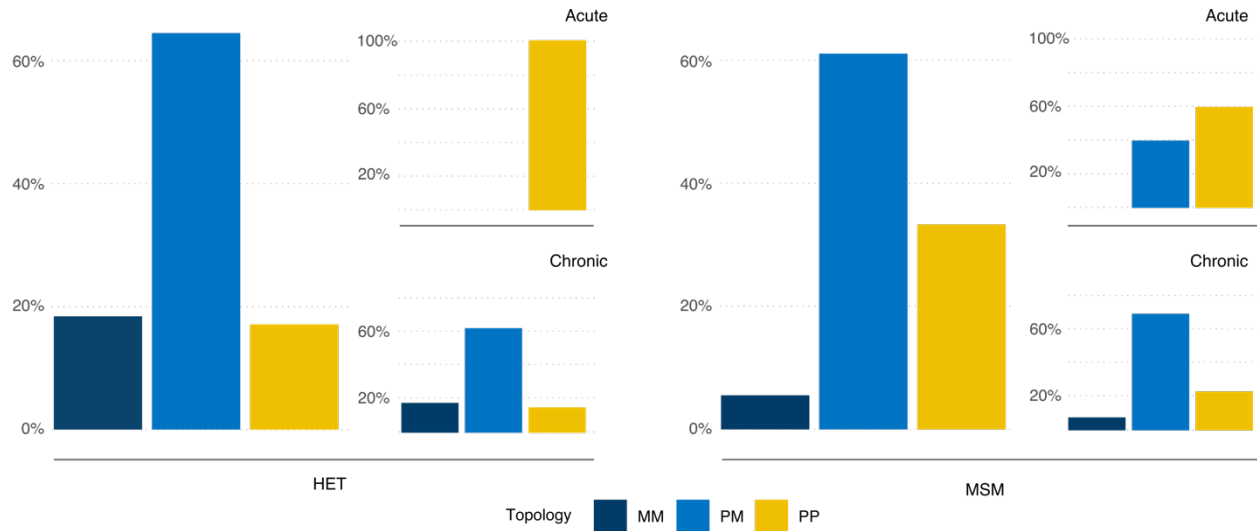
89 **Fig. 1: Methods schematics.** A) Phylogenetic tree topology class of known transmission pairs that have
 90 previously been used as a proxy for calculating the minimum number of founder variants transmitted to

91 the recipient: trees of class MM and PM both suggest a minimum of one founder variant while trees of
92 class PP suggest a multiple founder variants, with the minimum number of founder variants being the
93 number of recipient clades embedded in PP trees (here shown as two). B) Pipeline of phylodynamic
94 analysis (LANLdb, Los Alamos National Laboratory HIV sequence database) where teal represents data
95 or analysis output and white represents methods and analysis. An example of a standardised transmission
96 timeline for a known source-recipient pair is provided in panel C. C) Schematic of the transmission pair
97 model simulation that shows the transmission and sampling timelines. The simulated number of virus
98 particles transmitted to the index case, and the source and recipient partners (n_I , n_S , n_R respectively) are
99 shown on the transmission events timeline.

100

101 We then performed Bayesian phylogenetic tree reconstruction on the genetic sequences of the
102 transmission pairs and classified the topology class of each tree in the posterior distribution as
103 monophyletic-monophyletic (MM), paraphyletic-monophyletic (PM) or paraphyletic-
104 polyphyletic (PP). The most likely topology class was PM (65% and 61% for HET and MSM,
105 respectively), but with a higher number of PP trees in the MSM group ($P=0.056$, **Fig. 2**). This
106 result has previously been reported as indicative of a higher number of founder variants for
107 MSM (18). However, when we stratify the topology class by whether the source partner was in
108 acute or chronic infection at the time of transmission, our results indicate that the infection stage
109 of the source is the primary driver for any observed differences in topology class. Specifically,
110 there is no difference between the HET and MSM groups in the PM/PP topology class ratio
111 when transmission occurs in the chronic stage of infection ($P=0.570$). Note that only one HET
112 transmission occurs during the acute stage, and the topology class for this pair is PP. These
113 results remain qualitatively consistent when only data were analysed from the 66% of

114 transmission pairs for whom the posterior trees gave a certainty of over 95% for the most
 115 frequent topology class (**Fig. S3**). These results indicate that infection stage of the source partner,
 116 and not risk group *per se*, influences the diversity bottleneck at transmission.
 117



118
 119 **Fig. 2: Phylogenetic findings from the empirical transmission pairs.** Fraction of phylogenetic tree
 120 topology class (MM: Monophyletic-Monophyletic, PM: Paraphyletic-Monophyletic and PP: Paraphyletic-
 121 Polyphyletic) where each tree topology class is classified as the most frequent topology class of each
 122 posterior distribution per transmission pair. Results are stratified by risk group: 76 heterosexual (HET)
 123 pairs and 36 men-who-have-sex-with-men (MSM) pairs) and infection stage of the source partner at
 124 transmission (11 acute pairs defined as <90d post infection and 101 chronic pairs defined as ≥90d post
 125 infection).

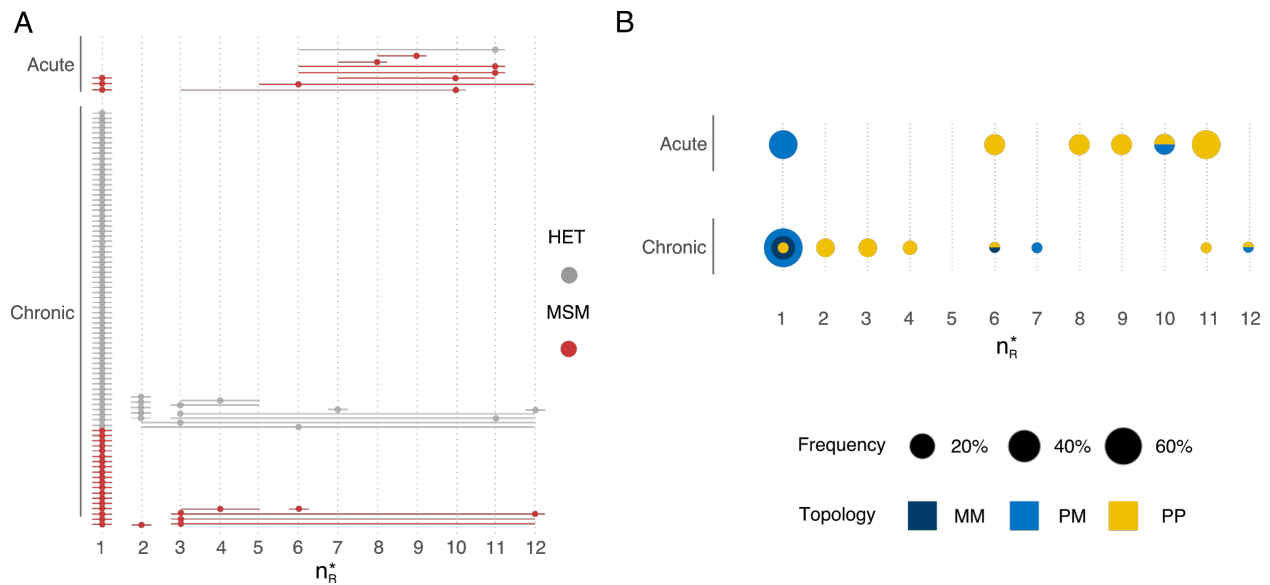
126 To test whether these empirical findings are indicative of a smaller diversity bottleneck in the
 127 chronic stage of HIV infection, we developed a phylodynamic framework in which we simulated
 128 the epidemiologic characteristics of each HET and MSM transmission pair, the timing of their
 129 sequence sampling, the transmission of virus particles, and the within-host genetic evolution in

130 both the source and recipient (**Fig. 1B**). Specifically, using the epidemiological information from
131 the transmission pairs, we simulated phylogenies under a coalescent model before generating
132 genetic sequences from these simulations and performing Maximum Likelihood (ML)
133 phylogenetic reconstruction on these simulated sequences. We classified each of these simulated
134 trees as MM, PM or PP and determined the frequency of each topology class (*i.e.* the fraction of
135 simulated trees that are classified as MM, PM and PP) for each simulated transmission pair
136 across all the simulated sequences. However, as we could not directly observe the number of
137 virus particles that are transmitted between source and recipient, we repeated the simulation of
138 phylogenetic trees for each transmission pair under a range of plausible values of virus particles
139 transmitted. By fitting the simulation output topology class distribution to the topology class
140 distribution from the empirical phylogenetic trees using maximum likelihood inference, we then
141 determined the most likely number of transmitted virus particles for each transmission pair and
142 used this best fit model for further analysis. Note that two or more virus particles may have the
143 same genetic sequence and would constitute a single founder variant (or haplotype), discussed
144 later. Further, due to the analysis conditioning on extant lineages, we use the term ‘founder
145 variants’ to describe those transmitted variants that found detectable viral lineages, thereby
146 ignoring variants that are transmitted but the lineages of which become extinct.

147 Our fitting procedure selects a best fit model that clearly delineates between transmission pairs
148 between whom one virus particle is transmitted (75% of pairs) and those between whom more
149 than one virus particle is transmitted (25% of pairs, **Fig. 3A**). While there is a high degree of
150 confidence in the result when one particle is transmitted, there is often uncertainty around the
151 exact number when multiple particles are transmitted (**Fig. 3A**). Importantly, we found acute
152 stage transmissions are more likely to lead to multiple particle infections compared with chronic

153 stage transmissions (73% vs. 20%, $P = 0.0005$). The topology class of the simulated
 154 phylogenetic trees is strongly influenced by the number of virus particles being transmitted (**Fig.**
 155 **3B**). PM trees are more commonly found in the pairs that are better described by a model with a
 156 single transmitted virus particle (81%) whereas PP trees appeared more often when multiple
 157 particles are likely to have been transmitted (86%).

158



159

160 **Fig. 3: The estimated number of transmitted virus particles for the 112 transmission pairs.** The
 161 estimates of transmitted virus particles for each transmission pair were calculated by choosing the model
 162 simulation that generated a phylogenetic tree topology class distribution (that is, the number of MM, PM
 163 and PP trees constructed from the simulated genetic sequences) that best matched the topology class
 164 distribution from the phylogenetic trees constructed from the empirical genetic sequences. A) Maximum
 165 likelihood number of virus particles founding recipient infections, n_R^* , for each pair (stacked points) with
 166 95% confidence intervals (lines) grouped by stage of infection (acute, 11 pairs or chronic, 101 pairs) and
 167 risk group (76 heterosexual pairs, HET and 36 men-who-have-sex-with-men pairs, MSM). B) Maximum

168 likelihood number of virus particles founding recipient infections coloured by topology class of the
169 phylogenetic tree constructed from the simulated genetic sequences.

170

171 For each transmission pair, we then simulated the genetic sequences of the transmitted viral
172 population under the best fit virus particle model and calculated the most likely number of
173 founder variants for each transmission pair (*i.e.* the number of distinct haplotypes). The median
174 number of founder variants transmitted across all pairs is 1 (range: 1-11, **Fig. 4A**). Using the full
175 distribution of the number of transmitted founder variants for each pair, we also calculated the
176 probability that a single founder variant was transmitted to the respective recipient. Our results
177 suggest that across all pairs in both risk groups, the mean probability of observing one founder
178 variant is 0.73. Stratifying by risk group, we find there is a higher probability that one founder
179 variant founds HET infections than MSM infections (a geometric mean of 0.80 vs. 0.63, **Fig.**
180 **4B**). However, these risk group differences mostly disappear when we stratify the results by the
181 infection stage of the source. Here, for example, when only chronic stage transmissions are
182 considered, there is no difference in the probability of one founder variant between MSM
183 transmissions and HET transmissions (means of 0.80 vs 0.71, $P=0.398$), and the pairwise
184 diversity at transmission is similar between both groups (**Fig. 4C**). In contrast, when stratifying
185 solely by infection stage of the source partner, we find that transmission during the acute stage
186 has a much lower probability of one founder variant than during the chronic stage (means of 0.40
187 vs. 0.77) with a higher median number of founder variants transmitted, when only the most likely
188 number of founder variants for each pair is considered (2 vs. 1, **Fig. 4A**). Nonetheless, if multiple
189 founder variant transmission does occur, our results suggest that the number of founder variants

190 is higher during chronic stage transmission, consistent with a higher diversity measure during
191 this later stage of infection (**Fig. 4C**).

192 From these results, therefore, there is approximately double the chance of multiple founder
193 variant transmission during acute stage infection across both risk groups (relative risk = 0.52).

194 Assuming that transmission risk is weighted towards early transmission such that half of all
195 index case to source partner transmissions occur after 90 days of index case infection leads to
196 qualitatively similar results (Supplementary Materials). Similarly, calibrating the simulation
197 model to bootstrapped samples rather than Bayesian posterior distributions leads to similar
198 results (Supplementary Materials).

199

200 Our results suggest that there is an association between tree topology class and multiple founder
201 variant transmission, with 95% of MM and PM trees being due to one founder variant (**Fig. 4D**).

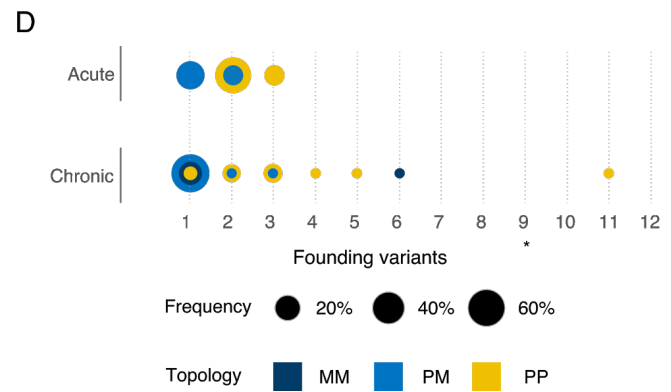
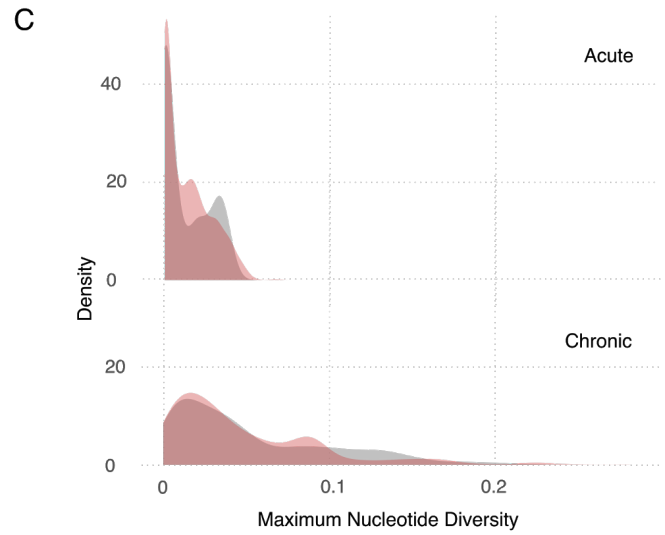
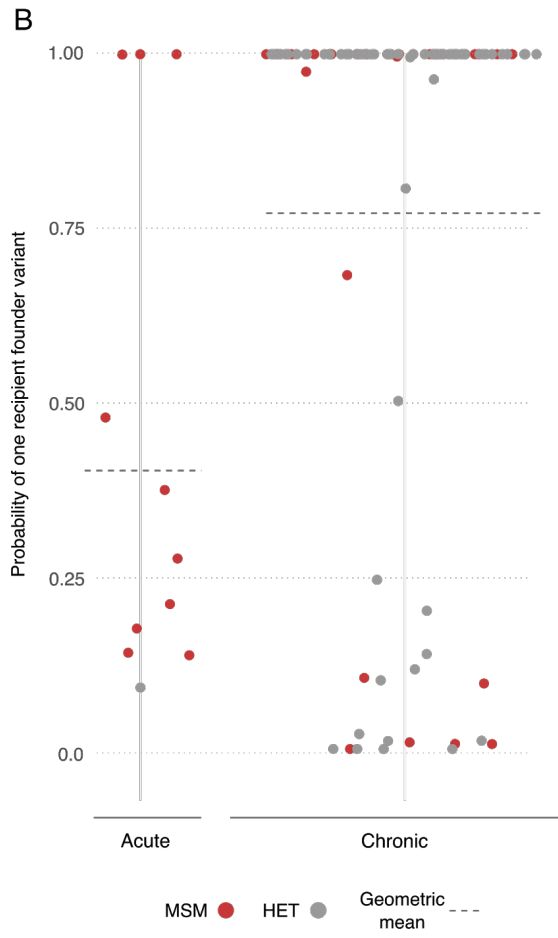
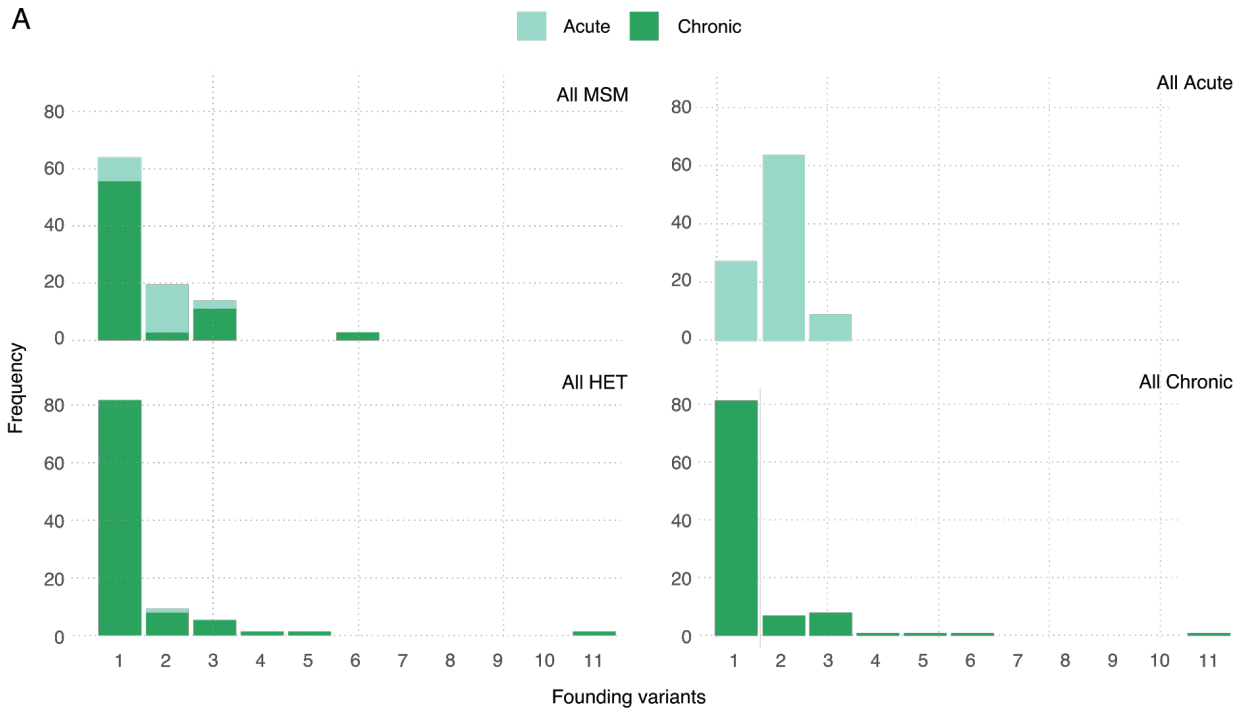
202 However, the number of embedded recipient clades is not always a proxy for the minimum
203 number of founder variants transmitted. For example, in chronic stage transmission, 11% of PP
204 topology class trees were due to single founder variant transmission (**Fig. 4D**). It is important to
205 stress that a PP topology class outcome may occur not only due to multiple genetically distinct
206 virus populations founding recipient infections but may also reflect a lack of phylogenetic signal
207 in the data; for instance, the sampled sequence lengths that gave rise to PP trees was on average
208 shorter than those for MM ($P=0.096$) and PM ($P=0.004$). Across both infection stages, we find
209 that if MM, PM or PP is assigned as the most likely tree topology class, then 92%, 96% and 15%
210 of transmissions are due to a single founder variant, respectively.

211

212 We have used a combination of empirical data and phylodynamic model simulation to evaluate
213 the role of infection stage at transmission and route of transmission on the number of virus
214 particles transmitted during sexual HIV exposure. This makes three important advances on
215 previous work. First, it is the first empirically-based study that fits a model to data to understand
216 the role of the source partner in multiple founder variant transmission. Second, while we use
217 previously developed topology classification of phylogenetic trees to understand HIV
218 transmission pairs, we extend this methodology by calibrating a phylodynamic model to
219 empirical data. This new approach provides a means to validate the untested assumption that the
220 number of embedded recipient partner lineages in a phylogenetic tree directly corresponds to the
221 minimum number of founder variants transmitted. Third, our phylodynamic model explicitly
222 incorporates virus particle number and the identity of genetic sequences. This advance produces
223 results that contrast with previous work that has shown the number of founder variants has little
224 impact on the topology class of the phylogenetic tree when only overall genetic diversity, rather
225 than sequence identity, is tracked (15).

226

227 The relative importance of acute and chronic stages of HIV in determining both the number of
228 virus particles and the number of founder variants transmitted is consistent with a recent
229 modelling study (14). However, our study finds higher proportions of infections initiated by
230 multiple founder variants overall during these two stages. This difference is likely due to the
231 assumptions related to how the stages of infection are defined as well as the relative importance
232 of transmission during late infection. Specifically, the previous modelling study finds that two
233 thirds of multiple founder variant transmission occurs during the pre-AIDS stage of infection
234 which is assumed to have both a high viral load and large haplotype diversity. If later stages of



236 **Fig. 4: Phylogenetic findings from the calibrated simulations.** A) Frequency of number of transmitted
237 founder variants for transmission pairs by either infection stage of source partner at transmission (left) or
238 risk group (right). The number of multiple founder variants is calculated as the modal simulated value. B)
239 Probability of one founder variant in the recipient for each pair stratified by infection stage of the source
240 partner at transmission. C) Probability density distribution of maximum diversity (proportion of sites that
241 differ) in the recipient partner across all simulations with more than one haplotype stratified by infection
242 stage of the source at transmission. D) Number of founder variants coloured by topology class of the
243 phylogenetic tree constructed from the best fit model of the simulated genetic sequences.

244

245 infection account for disproportionately less transmission than the previous model would predict
246 higher proportions of multiple founder variant transmission in both the acute and chronic stages
247 of infection, becoming more consistent with empirical estimates from our analysis. By contrast,
248 our study is agnostic about the relative importance of early and late transmission and does not
249 differentiate between chronic and a pre-AIDS stage of infection, which cannot easily be
250 identified through analysis of empirical data.

251

252 Data from four of the MSM transmission pairs in this study have previously been used to
253 estimate the number of variants founding infection using a combination approach of single
254 genome amplification (SGA), direct amplicon sequencing and mathematical modelling (7). Our
255 results broadly agree with this previous analysis, with both analyses suggesting two recipients
256 were infected with one founder variant and one recipient was infected with multiple founder
257 variants (our analysis suggests a mean of 2-3 founder variants and the previous analysis suggests
258 3 founder variants); there was disagreement with results from a fourth recipient, for whom a

259 single founder variant was 13% probable in this study (with a mode of 2 founder variants) but
260 the most likely outcome in the previous analysis. Small differences likely arise because this
261 study uses sequence data from both partners to evaluate the transmission of multiple founder
262 variants to the recipient partner. These extra data can be used to parameterize a mathematical
263 model that accounts for the evolutionary relationship between the virus samples from both
264 partners, rather than relying solely on accumulating diversity. Specifically, neglecting the extent
265 of genetic similarity between the source and recipient virus samples might misattribute
266 borderline cases of diversity accumulation.

267 Our study finds a median of one founder variant and a maximum of 11, with little difference
268 between HET and MSM risk groups. When only multiple founder variant transmissions are
269 considered, our study finds a median of 2-3 founder variants. These values are consistent with a
270 previous pooled analysis using results from four analyses that used the current gold-standard
271 SGA combination approach as above (9).

272 At present, the genetic determinants of HIV-1 disease progression are not clear. However, it is
273 important to note that even small differences between genotypes can have important clinical
274 outcomes. For instance, single polymorphisms can affect replication capacity (21), or can lead to
275 primary non-nucleoside reverse transcriptase inhibitor resistance with different amino acids
276 changes at the same position conferring equivalent levels of resistance (22).

277 Previous studies have disagreed over the extent to which the elevated risk of transmission during
278 the acute stage of infection (reviewed in (23)) is driven by increased viral load, elevated per
279 particle transmission probability or other behavioural factors such as high rates of sex partner
280 change or concurrent partnerships (24-29). Here, while we find strong evidence to support the

281 fact that acute stage transmissions are characterised by more virus particles and variants
282 founding infection, this result alone cannot disentangle virus- and host-related drivers of elevated
283 transmission. For example, the higher number of variants being transmitted during acute
284 infection could arise if the number of transmissible variants declines as infection progresses or,
285 because with more particles being transmitted, there are more opportunities for multiple variants
286 to found infection (14,30) However, our study can shed light on the eight times elevated per-
287 exposure risk of infection that has been found for MSM relative to HET transmission (31-32). In
288 particular, the lack of difference in both the number of virus particles and the number of founder
289 variants that establish infection after transmission from a chronically infected source in HET and
290 MSM suggests that the observed heightened acquisition risk for MSM could in part be due to
291 sampled MSM individuals being more likely to be in the acute stage at the time of transmission
292 (14, 27). Whether MSM partners are more likely to be sampled earlier in infection because of
293 sampling procedures or because MSM are indeed more likely to transmit during early infection is
294 unclear. While this observation raises the possibility that the role of sexual risk group in itself
295 may have less of an impact on the transmission of multiple founder variant probability, from a
296 pragmatic perspective, if more MSM infections are indeed caused by acute stage transmissions,
297 the evolutionary and epidemiologic impact on public health will be the same irrespective of the
298 mechanism.

299
300 There are two primary limitations to acknowledge. First, our model assumes a single
301 transmission event between each source and recipient partner. Without detailed knowledge of the
302 transmission pairs, we cannot distinguish between multiple infections each with a single founder
303 variant and a single infection with multiple founder variants; if for some pairs, the former were

304 true then this might suggest an elevated transmission rate during the acute stage, as has been
305 observed previously (28, 29). Second, our phylodynamic framework does not account for the
306 effect of selection and recombination. Specifically, selection, such as that for viruses which use
307 the CCR5 co-receptor (33), is thought to occur at the point of transmission , although the strength
308 may be dependent on the route of transmission (34).

309

310 Our study finds that the transmission of multiple HIV-1 founder variants is determined by
311 infection stage of the source partner, with transmission of more founder variants of HIV-1 in
312 acute compared with chronic infections. These findings stress that epidemiological or clinical
313 analysis of known transmission pairs should account for potential mediation by stage of
314 transmission when evaluating the effect of sexual risk group.

315

316 **Acknowledgements**

317 **Funding:** CJVA and KEA were funded by an ERC Starting Grant (award number 757688)
318 awarded to KEA. KAL was supported by The Wellcome Trust and The Royal Society grant no.
319 107652/Z/15/Z. MH was funded by The HIV Prevention Trials Network (grant number
320 H5R00701.CR00.01) and The Bill and Melinda Gates Foundation (grant number OPP1175094).

321 **Author contributions:** KEA conceived the study. CJVA, MH, KL, SH, KEA designed the
322 study. CJVA performed the experiments and analysed the data. CJVA, MH, KL, SH, KEA
323 interpreted the data. SGG created new software used in the study. KEA and CJVA drafted the
324 manuscript, with critical revisions from MH, RRR, KL, SH. All authors approved the final
325 version of the manuscript. **Competing interests:** The authors declare no competing interests.

326 **Data and materials availability:** All code and data are available at github.com/AtkinsGroup in

327 their respective repositories: data on the transmission pairs and sequence alignments
328 (TransmissionPairs_Data), code for retrieval of transmission pair epidemiological data and
329 metadata from Los Alamos National Laboratory HIV sequence database
330 (TransmissionPairs_LANLRetrieval), code for sequence retrieval from GenBank
331 (TransmissionPairs_GenBankRetrieval), code for phylodynamic analysis
332 (TransmissionPairs_PhyloDynamicAnalysis), and code for topological classification
333 (TransmissionPairs_TreeTopologyAnalysis).

334 **List of Supplementary Materials**

335 Materials and Methods

336 Supplementary Text

337 Figs. S1 to S5

338 Data S1 to S4

339 References (35-46)

340 Reproducibility Checklist

341

342 **References and Notes**

- 343 1. J. L. Geoghegan, A. M. Senior, E. C. Holmes, Pathogen population bottlenecks and
344 adaptive landscapes: overcoming the barriers to disease emergence. *Proc. Biol. Sci.*
345 283 (2016), doi:10.1098/rspb.2016.0727.
- 346 2. S. M. Kariuki, P. Selhorst, K. K. Ariën, J. R. Dorfman, The HIV-1 transmission
347 bottleneck. *Retrovirology*. 14 (2017), , doi:10.1186/s12977-017-0343-8.
- 348 3. K. Talbert-Slagle, K. E. Atkins, K.-K. Yan, E. Khurana, M. Gerstein, E. H. Bradley,
349 D. Berg, A. P. Galvani, J. P. Townsend, Cellular superspreaders: an epidemiological
350 perspective on HIV infection inside the body. *PLoS Pathog.* 10, e1004092 (2014).
- 351 4. B. F. Keele, E. E. Giorgi, J. F. Salazar-Gonzalez, J. M. Decker, K. T. Pham, M. G.
352 Salazar, C. Sun, T. Grayson, S. Wang, H. Li, X. Wei, C. Jiang, J. L. Kirchherr, F.
353 Gao, J. A. Anderson, L.-H. Ping, R. Swanstrom, G. D. Tomaras, W. A. Blattner, P. A.
354 Goepfert, J. M. Kilby, M. S. Saag, E. L. Delwart, M. P. Busch, M. S. Cohen, D. C.
355 Montefiori, B. F. Haynes, B. Gaschen, G. S. Athreya, H. Y. Lee, N. Wood, C.
356 Seoighe, A. S. Perelson, T. Bhattacharya, B. T. Korber, B. H. Hahn, G. M. Shaw,

- 357 Identification and characterization of transmitted and early founder virus envelopes in
358 primary HIV-1 infection. *Proc. Natl. Acad. Sci. U. S. A.* 105, 7552–7557 (2008).
- 359 5. J. F. Salazar-Gonzalez, E. Bailes, K. T. Pham, M. G. Salazar, M. B. Guffey, B. F.
360 Keele, C. A. Derdeyn, P. Farmer, E. Hunter, S. Allen, O. Manigart, J. Mulenga, J. A.
361 Anderson, R. Swanstrom, B. F. Haynes, G. S. Athreya, B. T. M. Korber, P. M. Sharp,
362 G. M. Shaw, B. H. Hahn, Deciphering human immunodeficiency virus type 1
363 transmission and early envelope diversification by single-genome amplification and
364 sequencing. *J. Virol.* 82, 3952–3970 (2008).
- 365 6. M.-R. Abrahams, J. A. Anderson, E. E. Giorgi, C. Seoighe, K. Mlisana, L.-H. Ping,
366 G. S. Athreya, F. K. Treurnicht, B. F. Keele, N. Wood, J. F. Salazar-Gonzalez, T.
367 Bhattacharya, H. Chu, I. Hoffman, S. Galvin, C. Mapanje, P. Kazembe, R. Thebus, S.
368 Fiscus, W. Hide, M. S. Cohen, S. A. Karim, B. F. Haynes, G. M. Shaw, B. H. Hahn,
369 B. T. Korber, R. Swanstrom, C. Williamson, CAPRISA Acute Infection Study Team,
370 Center for HIV-AIDS Vaccine Immunology Consortium, Quantitating the
371 multiplicity of infection with human immunodeficiency virus type 1 subtype C
372 reveals a non-poisson distribution of transmitted variants. *J. Virol.* 83, 3556–3567
373 (2009).
- 374 7. H. Li, K. J. Bar, S. Wang, J. M. Decker, Y. Chen, C. Sun, J. F. Salazar-Gonzalez, M.
375 G. Salazar, G. H. Learn, C. J. Morgan, J. E. Schumacher, P. Hraber, E. E. Giorgi, T.
376 Bhattacharya, B. T. Korber, A. S. Perelson, J. J. Eron, M. S. Cohen, C. B. Hicks, B.
377 F. Haynes, M. Markowitz, B. F. Keele, B. H. Hahn, G. M. Shaw, High Multiplicity
378 Infection by HIV-1 in Men Who Have Sex with Men. *PLoS Pathog.* 6, e1000890
379 (2010).
- 380 8. S. Gnanakaran, T. Bhattacharya, M. Daniels, B. F. Keele, P. T. Hraber, A. S.
381 Lapedes, T. Shen, B. Gaschen, M. Krishnamoorthy, H. Li, J. M. Decker, J. F. Salazar-
382 Gonzalez, S. Wang, C. Jiang, F. Gao, R. Swanstrom, J. A. Anderson, L.-H. Ping, M.
383 S. Cohen, M. Markowitz, P. A. Goepfert, M. S. Saag, J. J. Eron, C. B. Hicks, W. A.
384 Blattner, G. D. Tomaras, M. Asmal, N. L. Letvin, P. B. Gilbert, A. C. DeCamp, C. A.
385 Magaret, W. R. Schief, Y.-E. A. Ban, M. Zhang, K. A. Soderberg, J. G. Sodroski, B.
386 F. Haynes, G. M. Shaw, B. H. Hahn, B. Korber, Recurrent Signature Patterns in HIV-
387 1 B Clade Envelope Glycoproteins Associated with either Early or Chronic
388 Infections. *PLoS Pathogens.* 7 (2011), p. e1002209.
- 389 9. D. C. Tully, C. B. Ogilvie, R. E. Batorsky, D. J. Bean, K. A. Power, M.
390 Ghebremichael, H. E. Bedard, A. D. Gladden, A. M. Seese, M. A. Amero, K. Lane,
391 G. McGrath, S. B. Bazner, J. Tinsley, N. J. Lennon, M. R. Henn, Z. L. Brumme, P. J.
392 Norris, E. S. Rosenberg, K. H. Mayer, H. Jessen, S. L. Kosakovsky Pond, B. D.
393 Walker, M. Altfeld, J. M. Carlson, T. M. Allen, Differences in the Selection
394 Bottleneck between Modes of Sexual Transmission Influence the Genetic
395 Composition of the HIV-1 Founder Virus. *PLoS Pathog.* 12, e1005619 (2016).
- 396 10. K. A. Lythgoe, C. Fraser, New insights into the evolutionary rate of HIV-1 at the
397 within-host and epidemiological levels. *Proc. Biol. Sci.* 279, 3367–3375 (2012).
- 398 11. B. F. Keele, J. D. Estes, Barriers to mucosal transmission of immunodeficiency
399 viruses. *Blood.* 118 (2011), pp. 839–846.
- 400 12. L. R. McKinnon, R. Kaul, Quality and quantity. *Current Opinion in HIV and AIDS.* 7
401 (2012), pp. 195–202.

- 402 13. M. Sagar, Origin of the transmitted virus in HIV infection: infected cells versus cell-
403 free virus. *J. Infect. Dis.* 210 Suppl 3, S667–73 (2014).
- 404 14. R. N. Thompson, C. Wymant, R. A. Spriggs, J. Raghwani, C. Fraser, K. A. Lythgoe,
405 Link between the numbers of particles and variants founding new HIV-1 infections
406 depends on the timing of transmission. *Virus Evol.* 5 (2019), doi:10.1093/ve/vey038.
- 407 15. E. O. Romero-Severson, I. Bulla, T. Leitner, Phylogenetically resolving
408 epidemiologic linkage. *Proc. Natl. Acad. Sci. U. S. A.* 113, 2690–2695 (2016).
- 409 16. O. Ratmann, M. K. Grabowski, M. Hall, T. Golubchik, C. Wymant, L. Abeler-
410 Dörner, D. Bonsall, A. Hoppe, A. L. Brown, T. de Oliveira, A. Gall, P. Kellam, D.
411 Pillay, J. Kagaayi, G. Kigozi, T. C. Quinn, M. J. Wawer, O. Laeyendecker, D.
412 Serwadda, R. H. Gray, C. Fraser, PANGAEA Consortium and Rakai Health Sciences
413 Program, Inferring HIV-1 transmission networks and sources of epidemic spread in
414 Africa with deep-sequence phylogenetic analysis. *Nat. Commun.* 10, 1411 (2019).
- 415 17. C. Wymant, M. Hall, O. Ratmann, D. Bonsall, T. Golubchik, M. de Cesare, A. Gall,
416 M. Cornelissen, C. Fraser, STOP-HCV Consortium, The Maela Pneumococcal
417 Collaboration, and The BEEHIVE Collaboration, PHYLOSCANNER: Inferring
418 Transmission from Within- and Between-Host Pathogen Genetic Diversity. *Mol.*
419 *Biol. Evol.* 35, 719–733 (2018).
- 420 18. T. Leitner, E. Romero-Severson, Phylogenetic patterns recover known HIV
421 epidemiological relationships and reveal common transmission of multiple variants.
422 *Nat Microbiol.* 3, 983–988 (2018).
- 423 19. R. Rose, M. Hall, A. D. Redd, S. Lamers, A. E. Barbier, S. F. Porcella, S. E.
424 Hudelson, E. Piwowar-Manning, M. McCauley, T. Gamble, E. A. Wilson, J.
425 Kumwenda, M. C. Hosseinipour, J. G. Hakim, N. Kumarasamy, S. Chariyalertsak, J.
426 H. Pilotto, B. Grinsztejn, L. A. Mills, J. Makhema, B. R. Santos, Y. Q. Chen, T. C.
427 Quinn, C. Fraser, M. S. Cohen, S. H. Eshleman, O. Laeyendecker, Phylogenetic
428 Methods Inconsistently Predict the Direction of HIV Transmission Among
429 Heterosexual Pairs in the HPTN 052 Cohort. *J. Infect. Dis.* 220, 1406–1413 (2019).
- 430 20. A. B. Abecasis, M. Pingarilho, A.-M. Vandamme, Phylogenetic analysis as a forensic
431 tool in HIV transmission investigations. *AIDS.* 32, 543-554. (2017).
- 432 21. D. B. A. Ojwach, D. MacMillan, T. Reddy, V. Novitsky, Z. L. Brumme, M. A.
433 Brockman, T. Ndung’u, J. K. Mann, Pol-Driven Replicative Capacity Impacts
434 Disease Progression in HIV-1 Subtype C Infection. *J. Virol.* 92 (2018),
435 doi:10.1128/JVI.00811-18.
- 436 22. R. W. Shafer, J. M. Schapiro, HIV-1 drug resistance mutations: an updated
437 framework for the second decade of HAART. *AIDS Rev.* 10, 67–84 (2008).
- 438 23. W. C. Miller, N. E. Rosenberg, S. E. Rutstein, K. A. Powers, Role of acute and early
439 HIV infection in the sexual transmission of HIV. *Curr. Opin. HIV AIDS.* 5, 277–282
440 (2010).
- 441 24. E. M. Volz, E. Ionides, E. O. Romero-Severson, M.-G. Brandt, E. Mokotoff, J. S.
442 Koopman, *PLoS Med.*, 10(12): e1001568 (2013).
- 443 25. J. P. Hughes, J. M. Baeten, J. R. Lingappa, A. S. Magaret, A. Wald, G. de Bruyn, J.
444 Kiarie, M. Inambao, W. Kilembe, C. Farquhar, C. Celum, Partners in Prevention
445 HSV/HIV Transmission Study Team, Determinants of per-coital-act HIV-1
446 infectivity among African HIV-1-serodiscordant couples. *J. Infect. Dis.* 205, 358–365
447 (2012).

- 448 26. R. H. Gray, M. J. Wawer, R. Brookmeyer, N. K. Sewankambo, D. Serwadda, F.
449 Wabwire-Mangen, T. Lutalo, X. Li, T. vanCott, T. C. Quinn, Rakai Project Team,
450 Probability of HIV-1 transmission per coital act in monogamous, heterosexual, HIV-
451 1-discordant couples in Rakai, Uganda. *Lancet*. 357, 1149–1153 (2001).
- 452 27. T. D. Hollingsworth, R. M. Anderson, C. Fraser, HIV-1 transmission, by stage of
453 infection. *J. Infect. Dis.* 198, 687–693 (2008).
- 454 28. S. E. Bellan, J. Dushoff, A. P. Galvani, L. A. Meyers, Reassessment of HIV-1 acute
455 phase infectivity: accounting for heterogeneity and study design with simulated
456 cohorts. *PLoS Med.* 12, e1001801 (2015).
- 457 29. T. D. Hollingsworth, C. D. Pilcher, F. M. Hecht, S. G. Deeks, C. Fraser, High
458 Transmissibility During Early HIV Infection Among Men Who Have Sex With Men-
459 San Francisco, California. *J. Infect. Dis.* 211, 1757–1760 (2015).
- 460 30. K. A. Lythgoe, A. Gardner, O. G. Pybus, J. Grove, Short-Sighted Virus Evolution and
461 a Germline Hypothesis for Chronic Viral Infections. *Trends in Microbiology*. 25
462 (2017), pp. 336–348.
- 463 31. M.-C. Boily, R. F. Baggaley, L. Wang, B. Masse, R. G. White, R. J. Hayes, M. Alary,
464 Heterosexual risk of HIV-1 infection per sexual act: systematic review and meta-
465 analysis of observational studies. *Lancet Infect. Dis.* 9, 118–129 (2009).
- 466 32. R. F. Baggaley, R. G. White, M.-C. Boily, HIV transmission risk through anal
467 intercourse: systematic review, meta-analysis and implications for HIV prevention.
468 *Int. J. Epidemiol.* 39, 1048–1063 (2010).
- 469 33. M. Beretta, A. Moreau, M. Bouvin-Pley, A. Essat, C. Goujard, M.-L. Chaix, S. Hue,
470 L. Meyer, F. Barin, M. Braibant, ANRS 06 Primo Cohort, Phenotypic properties of
471 envelope glycoproteins of transmitted HIV-1 variants from patients belonging to
472 transmission chains. *AIDS*. 32, 1917–1926 (2018).
- 473 34. J. M. Carlson, M. Schaefer, D. C. Monaco, R. Batorsky, D. T. Claiborne, J. Prince,
474 M. J. Deymier, Z. S. Ende, N. R. Klatt, C. E. DeZiel, T.-H. Lin, J. Peng, A. M. Seese,
475 R. Shapiro, J. Frater, T. Ndung'u, J. Tang, P. Goepfert, J. Gilmour, M. A. Price, W.
476 Kilembe, D. Heckerman, P. J. R. Goulder, T. M. Allen, S. Allen, E. Hunter, HIV
477 transmission. Selection bias at the heterosexual HIV-1 transmission bottleneck.
478 *Science*. 345, 1254031 (2014).
- 479 35. M. S. Cohen, C. L. Gay, M. P. Busch, F. M. Hecht, The Detection of Acute HIV
480 Infection. *The Journal of Infectious Diseases*. 202 (2010), pp. S270–S277.
- 481 36. R. C. Edgar, MUSCLE: a multiple sequence alignment method with reduced time and
482 space complexity. *BMC Bioinformatics*. 5, 113 (2004).
- 483 37. R. C. Edgar, MUSCLE: multiple sequence alignment with high accuracy and high
484 throughput. *Nucleic Acids Res.* 32, 1792–1797 (2004).
- 485 38. F. Ronquist, J. P. Huelsenbeck, MrBayes 3: Bayesian phylogenetic inference under
486 mixed models. *Bioinformatics*. 19, 1572–1574 (2003).
- 487 39. J. P. Huelsenbeck, F. Ronquist, MRBAYES: Bayesian inference of phylogenetic
488 trees. *Bioinformatics*. 17, 754–755 (2001).
- 489 40. O. Ratmann, E. B. Hodcroft, M. Pickles, A. Cori, M. Hall, S. Lycett, C. Colijn, B.
490 Dearlove, X. Didelot, S. Frost, A. S. M. M. Hossain, J. B. Joy, M. Kendall, D.
491 Kühnert, G. E. Leventhal, R. Liang, G. Plazzotta, A. F. Y. Poon, D. A. Rasmussen, T.
492 Stadler, E. Volz, C. Weis, A. J. Leigh Brown, C. Fraser, PANGAEA-HIV Consortium,

- 493 Phylogenetic Tools for Generalized HIV-1 Epidemics: Findings from the PANGEA-
494 HIV Methods Comparison. *Mol. Biol. Evol.* 34, 185–203 (2017).
- 495 41. A. Rambaut, N. C. Grassly, Seq-Gen: an application for the Monte Carlo simulation
496 of DNA sequence evolution along phylogenetic trees. *Comput. Appl. Biosci.* 13, 235–
497 238 (1997).
- 498 42. S. Alizon, C. Fraser, Within-host and between-host evolutionary rates across the
499 HIV-1 genome. *Retrovirology.* 10, 49 (2013).
- 500 43. L.-T. Nguyen, H. A. Schmidt, A. von Haeseler, B. Q. Minh, IQ-TREE: a fast and
501 effective stochastic algorithm for estimating maximum-likelihood phylogenies. *Mol.*
502 *Biol. Evol.* 32, 268–274 (2015).
- 503 44. S. Kalyaanamoorthy, B. Q. Minh, T. K. F. Wong, A. von Haeseler, L. S. Jermiin,
504 ModelFinder: fast model selection for accurate phylogenetic estimates. *Nat. Methods.*
505 14, 587–589 (2017).
- 506 45. S. R. Cole, H. Chu, S. Greenland, Maximum likelihood, profile likelihood, and
507 penalized likelihood: a primer. *Am. J. Epidemiol.* 179, 252–260 (2014).
- 508 46. S. S. Iyer, F. Bibollet-Ruche, S. Sherrill-Mix, G. H. Learn, L. Plenderleith, A. G.
509 Smith, H. J. Barbian, R. M. Russell, M. V. P. Gondim, C. Y. Bahari, C. M. Shaw, Y.
510 Li, T. Decker, B. F. Haynes, G. M. Shaw, P. M. Sharp, P. Borrow, B. H. Hahn,
511 Resistance to type 1 interferons is a major determinant of HIV-1 transmission fitness.
512 *Proc. Natl. Acad. Sci. U. S. A.* 114, E590–E599 (2017).
- 513

1
2
3
4
5
6
7
8
9
10
11
12
13
14
15
16
17
18
19
20
21
22
23
24
25

Supplementary Materials for:

Number of HIV-1 founder variants is determined by the recency of the source partner infection

Ch. Julián Villabona-Arenas, Matthew Hall, Katrina A. Lythgoe, Stephen G. Gaffney, Roland R. Regoes, Stéphane Hué, Katherine E. Atkins

Correspondence to: Katherine.Atkins@ed.ac.uk

This PDF file includes:

- Materials and Methods
- Supplementary Text
- Figs. S1 to S5
- Additional references

Other Supplementary Materials for this manuscript include the following:

- Data S1 to S4: SITable_EpiGeneticData.csv, SITable_AnalysisData.csv, SITable_ColumnNamesKey.csv, Alignments.zip, Reproducibility checklist

Materials and Methods

Data collation on linked transmission pairs

We automatically retrieved all HIV sequence data for men-who-have-sex-with-men (MSM) and heterosexual (HET) HIV transmission pairs for whom the direction of transmission is reported from The Los Alamos National Laboratory (LANL) HIV sequence database up to February

26 2019, such that each transmission pair comprise a ‘source’ and a ‘recipient’ partner. For each
27 partner in the transmission pair we collected the following clinical and epidemiological data: (i)
28 date of infection or time of infection prior to sampling, (ii) date of seroconversion or date of
29 seroconversion prior to sampling, (iii) Fiebig stage at the time of sampling, (iv) date of sampling
30 or time of sampling prior to infection, (v) number of sequences, (vi) genomic region, (vii) HIV
31 subtype, and (viii) reported risk group. For each set of these transmission pair data we estimated,
32 relative to the transmission time to the recipient partner (time = 0): (i) the time of transmission to
33 the source partner, (ii) the time of the sampling of the source partner, and (iii) the time of
34 sampling for the recipient partner (**Fig. 1**, Supplementary Text). We excluded all transmission
35 pairs from further analysis for whom these three times could not be determined or for whom
36 either partner has fewer than five sequences for all sampling times. For our base case analysis,
37 we used the longest available genomic region with five or more sequences per partner. If more
38 than one sampling time is available for any of the individuals, we selected the sample closest in
39 time to the recipient infection.

40 **Epidemiological data and sequence retrieval**

41 For the ease of replicating our results and using existing transmission pair data for other
42 purposes, we developed a Python script to automatically retrieve epidemiological and metadata
43 for each transmission pair from the Los Alamos National Laboratory HIV sequence database
44 (LANLdb). This script downloads the following data from both the source and recipient partners
45 to a .csv file using as input the cluster and patients ids from LANLdb: (i) time of infection, (ii)
46 time of seroconversion, (iii) Fiebig stage at the time of sampling, (iv) number of sequences, (v)
47 genomic region, (vi) HIV subtype, (vii) reported risk group and (viii) GenBank accession IDs.

48

49 Next we used the downloaded GenBank accession IDs to automatically retrieve (ix) viral genetic
50 sequences and (x) sampling dates (calendar dates) from GenBank using an R script. If
51 information from (i) to (x) were missing for any individual, we manually retrieved these values
52 from the original manuscripts where possible.

53

54 Completed datatables from these automatic and manual processes are provided at
55 github.com/AtkinsGroup.

56

57 **Transmission timelines**

58 For each transmission pair, we define time = 0 as the time of recipient infection. We then
59 calculated, using the data table retrieved, i) the time of infection of the source, ii) the time of
60 sampling of the source, iii) the time of sampling of the recipient.

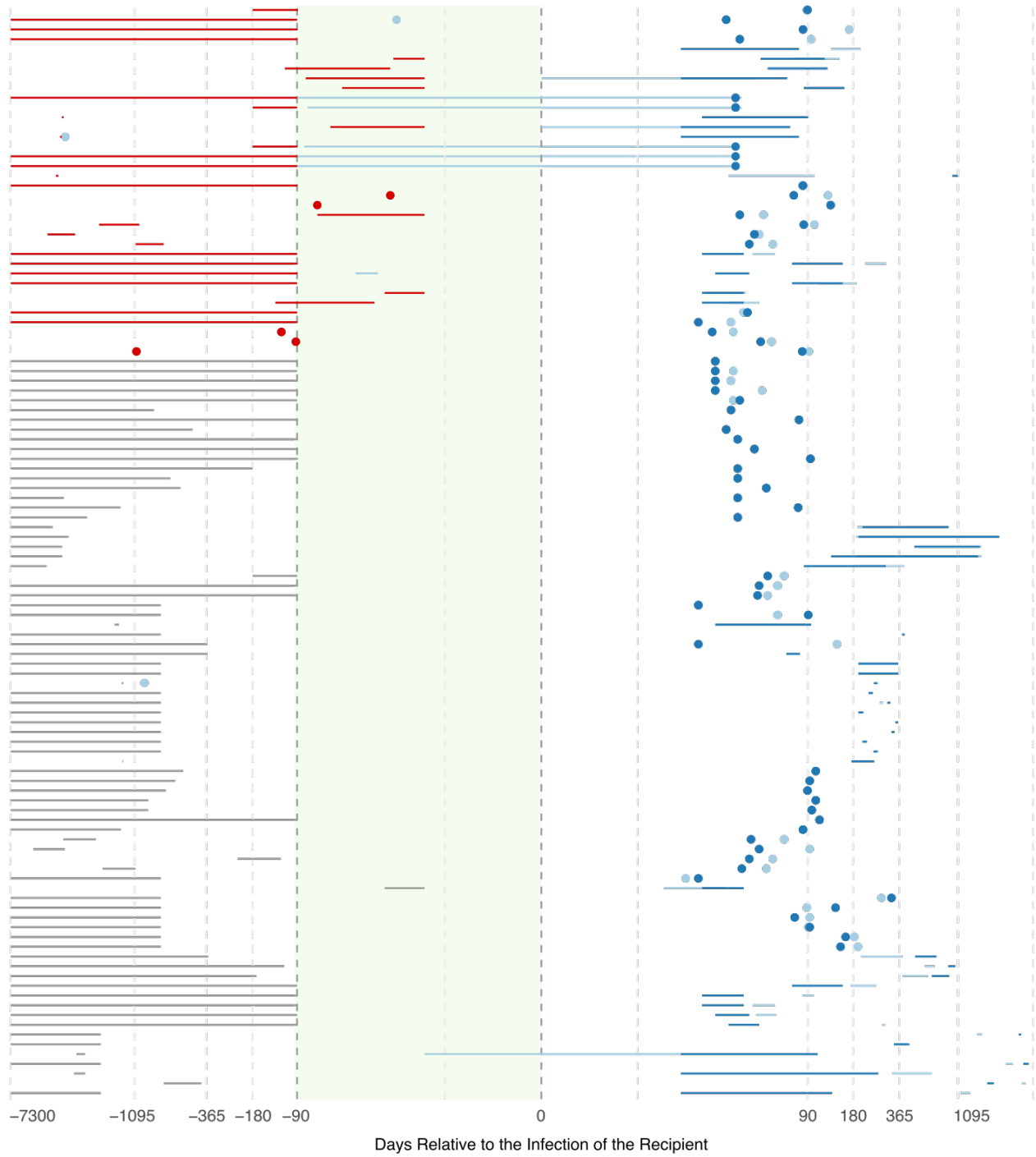
61

62 To estimate these times, we first calculated days from infection for both the source and the
63 recipient partners. When these values are not given explicitly, we calculated them from time
64 since seroconversion estimates or from Fiebig staging results. Specifically, we interpret
65 seroconversion as the individual reaching Fiebig stage III (ELISA positive) that occurs between
66 22-37 days after infection and Fiebig stages I (viral RNA positive) and II (18-34) occurring 13
67 days and 28 days after infection, respectively (35). For all the pairs where a range of possible
68 values is calculated, and for when a calendar month is provided, we incorporated the uncertainty
69 around the infection and sampling times by assuming all values in these ranges are equally
70 plausible and uniformly sampled within these range to account for the uncertainty.

71

72 For some pairs, the source was classified as ‘recent’ or ‘late’ at the time of transmission to the
73 recipient partner. In these cases, we do not have an exact point to call time = 0. Therefore, for
74 these pairs, for each simulation, we sample with replacement the time between source and
75 recipient infections from the other pairs for whom we have previously classified as acute (<90
76 days delay), and chronic (90 days or more delay), sampling from the same risk group (MSM or
77 HET) in each case.

78 All calculations, corresponding notes and final transmission times for each pair are provided at
79 github.com/AtkinsGroup and visualised in **Fig. S1**.



80



81 **Fig. S1: Infection and sampling times of the source and recipient for all the 112 transmission pairs**

82 **analysed.** Individual points denote exact times and lines denote uniform uncertainty in times. Source

83 partners points/lines overlapping the green shaded area correspond to transmission pairs for whom
84 transmission occurs during the acute stage.

85

86 **Empirical transmission pair analysis**

87 *Tree reconstruction:* For each of the included transmission pairs, we generated posterior sets of
88 phylogenetic trees. For this, we first constructed alignments using Muscle v3.8.31 (36, 37) with
89 subtype specific reference sequences retrieved from the LANL HIV sequence database. Using
90 these alignments, we built phylogenetic trees with MrBayes 3.2.7 (38, 39) under the assumption
91 of a general time-reversible (GTR) nucleotide substitution model with the addition of invariant
92 sites (I) and a gamma distribution of site rates. We constrained sequence data to be monophyletic
93 with respect to the reference sequences to root the tree but ingroup relationships were
94 unconstrained to avoid any topology class bias. We ran two Markov chains each with 30 million
95 iterations, from which we sampled every 3,000th after discarding the first 50% as burn-in which
96 provided an average standard deviation of split tree frequencies of below 0.01 or an effective
97 sample size of greater than 300. This gave an empirical posterior distribution of $N = 5,000$
98 sample trees. In a sensitivity analysis, we tested the alternative method of using maximum
99 likelihood phylogenetic tree reconstruction with bootstrapping.

100

101 *Empirical topology class:* We classified each of the resulting phylogenetic trees in the posterior
102 distribution as either monophyletic-monophyletic (MM), or paraphyletic-monophyletic (PM), or
103 paraphyletic-polyphyletic (PP), to reflect the cladistic relationship between the lineages from
104 both individuals (Supplementary Text). Each transmission pair, k , is then described as a triplet of
105 probabilities, D_k , denoting the frequency of each topology class within the k th pair's posterior

106 distribution $D_k = \{d_k(t)\}_{t \in T} = \{\Pr(t | k)\}_{t \in T}$ where $\sum_{t \in T} \Pr(t | k) = 1$ and $T \in$
107 $\{\text{MM, PM, PP}\}$.

108

109 **Simulated transmission pair analysis**

110 We simulated the transmission of virus particles and within-host evolution, accounting for the
111 epidemiological characteristics for each transmission pair. For each transmission pair, we
112 simulated a chain of three HIV infections: (i) an unsampled index case who infected the source
113 after three years of their own infection during their chronic stage to reflect that the majority of
114 both HET and MSM transmission pairs transmitted during the chronic stage (101/112 pairs). In a
115 sensitivity analysis we accounted for the assumption that transmission rate may be higher during
116 the acute stage, with half of the index to source transmissions occurring after 90 days and the
117 remaining half after three years, (ii) the source individual of the transmission pair, and (iii)
118 finally the recipient individual of the transmission pair. For each individual within each trio, we
119 simulated viral phylogenies that reflect between- and within-host viral evolution using
120 VirusTreeSimulator (40), using as input the respective epidemiological and clinical information
121 (Supplementary Text). We used a within-host effective population size consistent with that
122 parameterized by the PANGEA-HIV study with the following logistic model parameters: initial
123 effective population size (N_0) is 1, viral generation time (τ) is 1.8 days, effective population per
124 year growth rate (r) is 2.85022, and time to half the carrying capacity of the viral population
125 (t_{50}) is 2 years (40). For each transmission pair, we simulated a dated viral phylogeny that has
126 the same number of tips as the number of retrieved sequences per partner and that is sampled at
127 the respective sampling times for the source and recipient partner (Supplementary Text). For
128 each recipient partner infection, we assume that a total of n_R virus particles founded the

129 infection. For each simulation, we further assume a total of n_S virus particles founding infection
130 of the source. We assume n_R takes values between one and a maximum of 12 and varied n_S
131 between one and two (Supplementary Text). We assume that the virus samples from each
132 recipient is representative of the within-host diversity, and that each founding virus particle has
133 an extant lineage. Therefore, we first assigned each sample (tip) of a phylogeny as a descendant
134 of one of the n_R virus particles. If there were more than 12 samples then the remaining tips were
135 assigned randomly to the $n_R = 12$ virus particles. If there were fewer than 12 samples, then we
136 constrained the number of founding virus particles, n_R , to equal the number of samples. For
137 every transmission pair, and for each value of n_R and n_S , we simulated 100 viral phylogenies.

138

139 For every simulated viral phylogeny, we simulated transmitted sequences by adding dummy
140 nodes with a negligibly short branch length after the transmission time. We then simulated the
141 evolution of nucleotide sequences along the tree using Seq-Gen (41) and a GTR + I + gamma
142 substitution model. The length of the simulated sequences and the evolutionary tree scaling rate
143 match each transmission pair's empirical sequence data. For this, we used previously estimated
144 empirically-derived within-host evolutionary rates (42) and the HXB2 sequence homologous to
145 the pair's sequence fragment as the ancestral sequence at the root. Every transmission pair
146 simulation produces a tip sequence alignment and a number of founder sequences equal to the
147 number of transmitted particles.

148

149 *Simulated topology class:* We reconstructed a phylogeny using maximum likelihood inference in
150 IQ-TREE 1.6.11 (43) and selected the best-fit nucleotide substitution model with ModelFinder
151 (44). Each phylogeny was classified as either MM, PM or PP (Supplementary Text).

152 Consequently, for each transmission pair k and each transmissibility model (i.e. number of viral
 153 particles founding infection of the recipient n_R), we generated a triplet of probabilities $M_{k,n_R} =$
 154 $\{m_{k,n_R}\}_{t \in T} = \Pr(t|k, n_R)$ where $\sum_{t \in T} \Pr(t|k, n_R) = 1$ and $T \in \{\text{MM, PM, PP}\}$.

155

156 **Transmissibility model calibration**

157 For each transmission pair, we chose the most likely value of n_R (the number of virus particles
 158 founding each recipient infection) by matching the posterior topology class from the empirical
 159 phylogenetic transmission trees with the simulated distribution of topology class. Specifically,
 160 for each transmission pair, k , we estimated the most likely number of viral particles founding
 161 each recipient infection n_R^* as the n_R that maximises the multinomial likelihood function $L_{k,n_R} =$

162 $\Pr(D_k | M_{k,n_R}) = \frac{N!}{\prod_{t \in T} (N d_k(t))!} \prod_{t \in T} m_{k,n_R}(t)^{N d_k(t)}$. For each transmission pair k , we calculated

163 lower and upper confidence limits for n_R^* as the minimum and maximum values of n_R that satisfy

164 $L_{k,n_R} > L_{k,n_R^*} - 1.92$ and $L_{k,n_R} < L_{k,n_R^*} + 1.92$, respectively (44, 45). For each transmission

165 pair k , we retain the best fit model for further analysis such that there are n_R^* viral particles

166 founding infection of the recipient.

167 **Haplotype analysis**

168 *Probability of a single founder haplotype:* For each transmission pair, k , from the best fit

169 transmissibility model, we defined the random variables F_S^k and F_R^k as the number of haplotypes

170 that found infection of the source and the recipient partners, respectively. We then calculated the

171 probability of there being a single founder haplotype in the recipient, stratified by topology class

172 of the simulated phylogenetic tree (MM, PM, PP) and the number of founder haplotypes, i , in the

173 source partner, $p_i^k(t)$, that is, $p_i^k(t) = \Pr(F_R^k = 1 | F_S^k = i, t)$. Next, we defined the probability
 174 of a single founder haplotype in the recipient as a function of a tree topology, t , $p^k(t) =$
 175 $\Pr(F_R^k = 1 | t) = p_1^k \Pr(F_S = 1) + p_2^k \Pr(F_S > 1)$. By assuming that the source partners are
 176 randomly selected from the general MSM or HET population in which the probability of a single
 177 founder variant has been calculated to be approximately 0.7 (14), we set, $\Pr(F_S = 1) =$
 178 0.7 and $\Pr(F_S > 1) = 0.3$. Finally, for each transmission pair, we calculated the probability of
 179 one founder haplotype given the observed triplet of empirical posterior topology classes D_k , as
 180 $q^k = \sum_{t \in T} p^k(t) d_k(t) / N$.

181
 182 *Number of founder haplotypes by source partner infection stage:* We stratified all the
 183 transmission pairs into two sets by the infection stage of the source partner. We classified the
 184 acute transmission set as those pairs for whom recipient infection is within 90 days of source
 185 infection (a set of n_{acute} pairs), and the chronic transmission set as those pairs for whom recipient
 186 infection is 90 days or later after source infection (a set of n_{chronic} pairs). For each group, we
 187 calculated the mean probability of one founder haplotype being transmitted to the recipient in
 188 each set set as:

$$189 \quad q_{\text{acute}}^k = \sqrt[n_{\text{acute}}]{\prod_{k \in \text{acute}} q^k}$$

$$190 \quad q_{\text{chronic}}^k = \sqrt[n_{\text{chronic}}]{\prod_{k \in \text{chronic}} q^k}$$

191 Finally, we calculated the relative risk of one founder haplotype transmitted during the acute
 192 stage versus the chronic stage by $q_{\text{acute}}^k / q_{\text{chronic}}^k$.

193 **Statistical analysis**

194 We compare our results by using statistical tests and report the respective *P*-values. To compare

195

196

197

198

199 **Supplementary Text**

200

201 **Transmission pairs sequence data**

202 Our alignments are provided at github.com/AtkinsGroup.

203 On average, 22 (IQR 13-33) HIV sequences are obtained from the source and 21 (IQR 10-20)

204 sequences from the recipient for the MSM pairs, and 21 (IQR 12-25) and 18 (IQR 9-22) for the

205 HET source and recipient, respectively. All MSM sequence data belong to subtype B, while most

206 heterosexual sequence data belong to subtype C (49%), followed by subtype B (22%), subtype D

207 (21%), subtype A/A-like (7%) and unclassified subtype (1%). A total of 7 (19%) of the MSM

208 pairs have near full genomes sequenced and the remaining pairs had *env* available (mean 1653

209 nt, range 182-3827 nt). Ten (13%) of the HET pairs had near full genomes available, while 56

210 (75%) pairs had *env* (mean 1321 nt, range 323-2582 nt), nine (12%) pairs had either *pol* or *gag*

211 (mean 1484 nt, range 1375-1499 nt) and one pair had *vif*-LTR3 (4666 nt) sequenced.

212

213 **Effect of number of founding virus particles in the source**

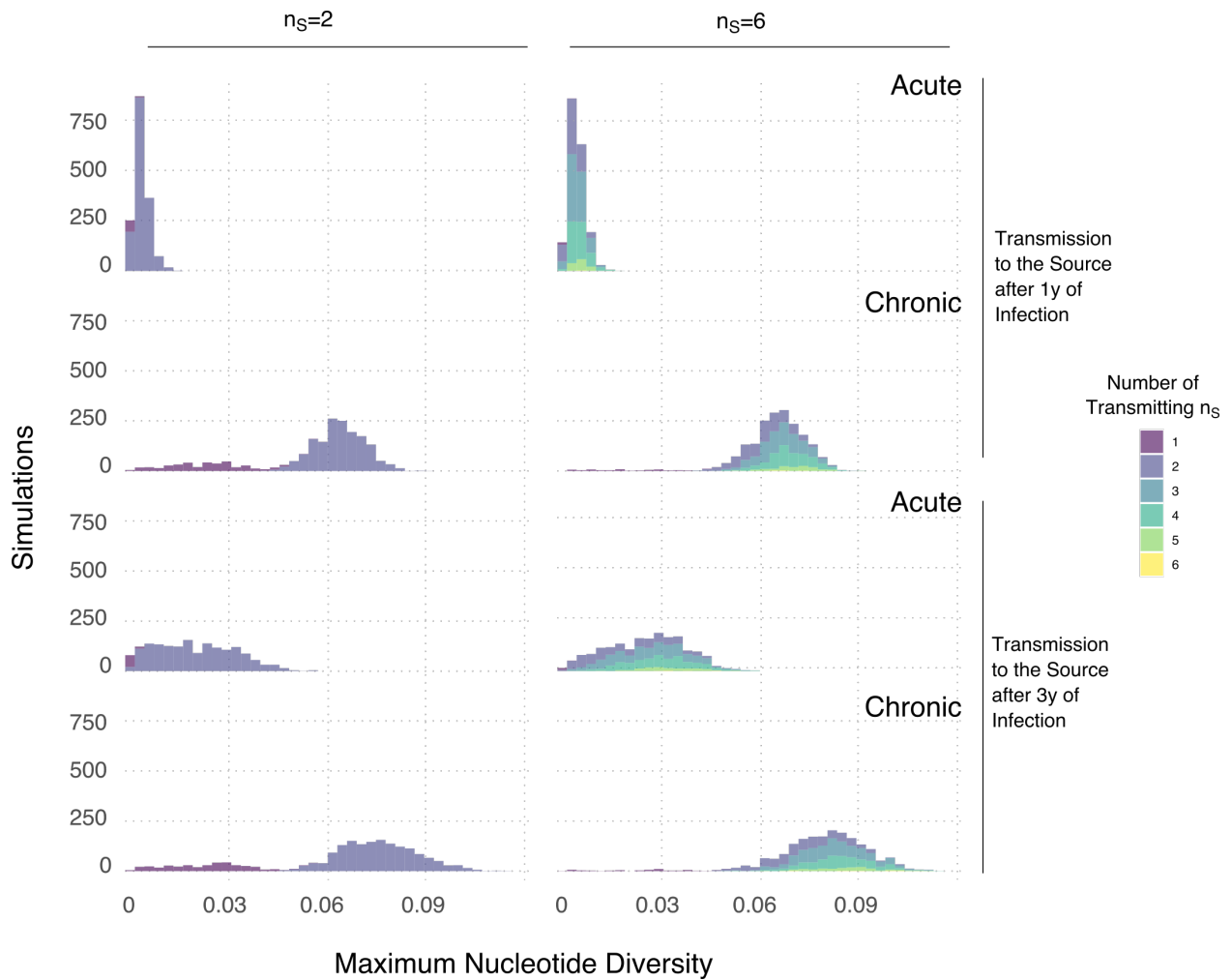
214 To assess whether the number of founding virus particles in the source partner affects the
215 diversity of sequences founding infection in the recipient, we model a scenario where the index
216 case transmitted one, two or six virus particles to the source partner at either one or three year(s)
217 after infection. The source in turn transmits 1 to 6 virus particles to the recipient at 30 days
218 (acute) or 1095 days (chronic) later. The simulation produces a dated viral phylogeny with tips
219 sampled at either 30 (early) or 1065 days (late). We model 1kb nucleotide sequences along the
220 simulated viral phylogenies using the same method as in the main text.

221

222 The genetic variation rapidly and steadily increases over time – the maximum diversity among
223 transmitted haplotypes to the recipient was higher when the index case was infected for longer
224 and the transmission to the recipient occurs during the chronic stage of the source (**Fig. S2**).

225 When the source has more than one founding particle, this leads to a bimodal distribution of
226 maximum diversity among transmitted founder variants within the recipient. The first and second
227 mode represent maximum diversity when drawing the recipient founder haplotypes from either
228 one or more than one viral population within the source, respectively. However, increasing the
229 number of founding virus particles to more than two within the source only increases the density
230 around the second mode without affecting the range of the maximum diversity distribution. This
231 consistency occurs because increasing the number of founding virus particles in both
232 transmission partners, increased the probability of drawing founding variants from different
233 genetic pools in the source. However, the average maximum diversity of the founder variants

234 does not change because the source genetic pools evolved at the same rate and under the same
 235 evolutionary constraints with no selective advantage. This leads to genetic pools with equivalent
 236 cumulative genetic change but distinct identity. Taking this into account, we chose to model one
 237 or two founding virus particles within the source partner as we were interested in capturing some
 238 degree of variation in the transmitted haplotypes rather than multiple genetic identities *per se*.



239

240 **Fig. S2: Effect of number of founding virus particles in the source.**

241

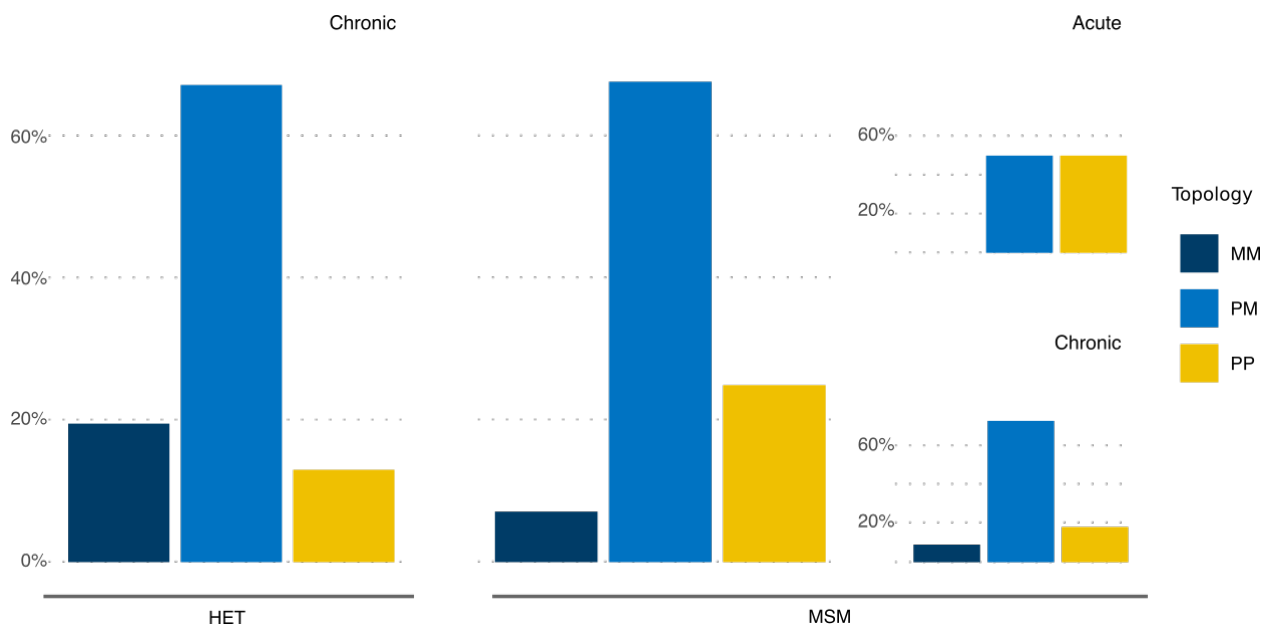
242

243

244

245

246 **Effect of using a confidence threshold for assigning the topology class**



247

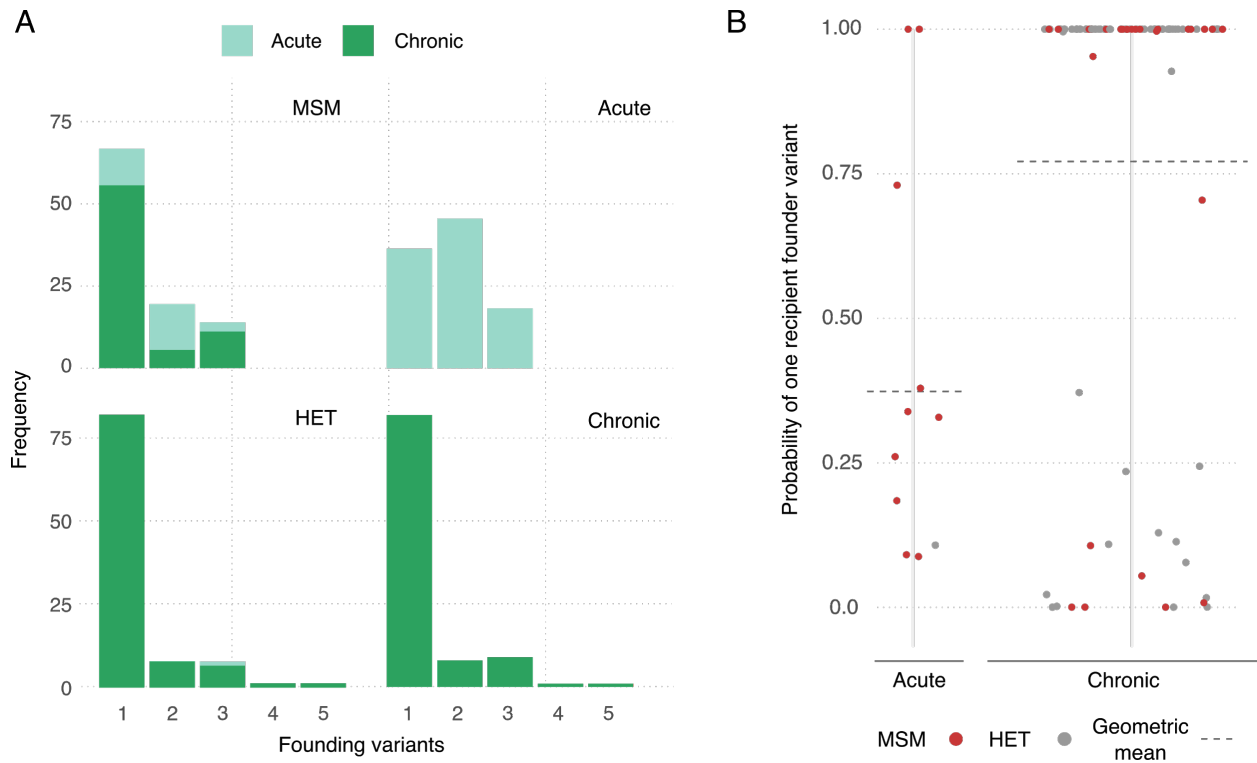
248 **Fig. S3: Phylogenetic findings of the empirical transmission pairs for whom the posterior trees**
 249 **gave a certainty of over 95% for the most frequent topology.** Fraction of phylogenetic tree topology
 250 class (MM - Monophyletic-Monophyletic, PM - Paraphyletic-Monophyletic and PP - Paraphyletic-
 251 Polyphyletic) where each tree topology class is classified as the most frequent topology class of each
 252 posterior distribution per transmission pair. Results are stratified by risk group: 76 heterosexual (HET)
 253 pairs and 36 men-who-have-sex-with-men (MSM) pairs) and infection stage of the source partner at
 254 transmission (11 acute pairs defined as <90d post infection and 101 chronic pairs defined as ≥90d post
 255 infection).

256

257 **Effect of index partner stage of infection at transmission**

258 In the main analysis we assumed that all index cases transmit to the source partner after three
259 years of infection. Here we also evaluated the results assuming the transmission risk was skewed
260 towards early infection, with half of all simulations across all transmission pairs assuming index
261 case transmission occurs during the acute stage (≤ 90 d) and half occurs during the chronic stage
262 (91d-3y). We find qualitatively similar results as our main analysis. The median number of
263 founder variants transmitted across all pairs is 1 (range: 1-5, **Fig. S4A**). Across all pairs in both
264 risk groups, the mean probability of observing one founder variant is 0.73. Stratifying by risk
265 group, we find there is a higher probability that one variant founds HET infections than MSM
266 infections (a geometric mean of 0.79 vs. 0.61, **Fig. S4B**). In contrast, when stratifying solely by
267 infection stage of the source partner, we find that transmission during the acute stage has a much
268 lower probability of one founder variant than during the chronic stage (means of 0.38 vs. 0.78)
269 with a higher median number of founder variants transmitted, when only the most likely **number**
270 **of transmitted founder variants** for each pair is considered (2 vs. 1, **Fig. S4A**). From these results,
271 therefore, there is still approximately twice the chance of multiple founder variant transmission
272 during acute stage infection across both risk groups (relative risk is 0.48).

273



274

275 **Fig. S4: Phylogenetic findings from the calibrated simulations with skewed transmission rate**

276 **towards acute stage for the index case.** A) Frequency of the number of founder variants for

277 transmission pairs by infection stage of source partner at transmission and risk group. The **number of**

278 **transmitted founding variants** is calculated as the modal simulated value. B) Probability of one founder

279 variant in the recipient for each pair stratified by infection stage of the source partner at transmission.

280

281 **Effect of constructing empirical data phylogenetic trees using maximum likelihood**

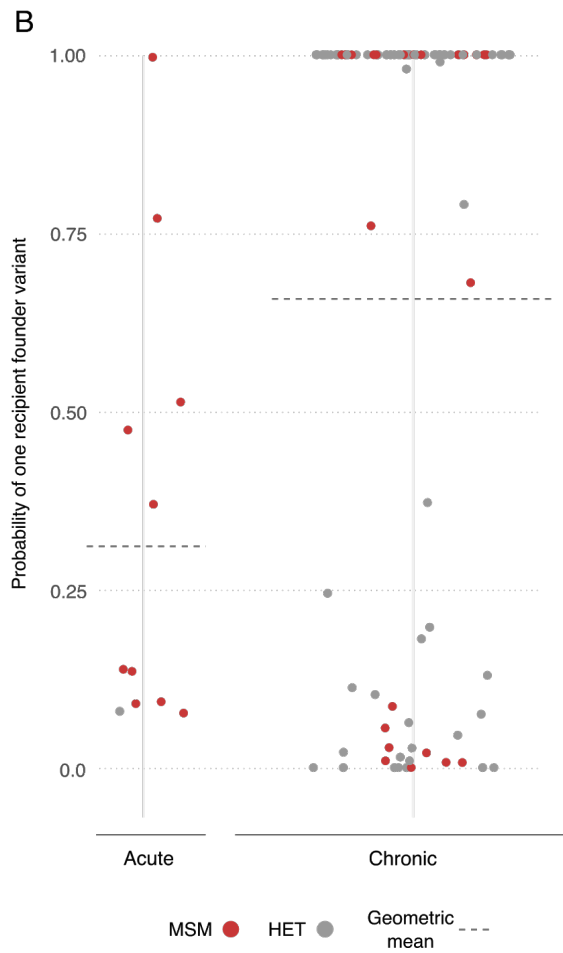
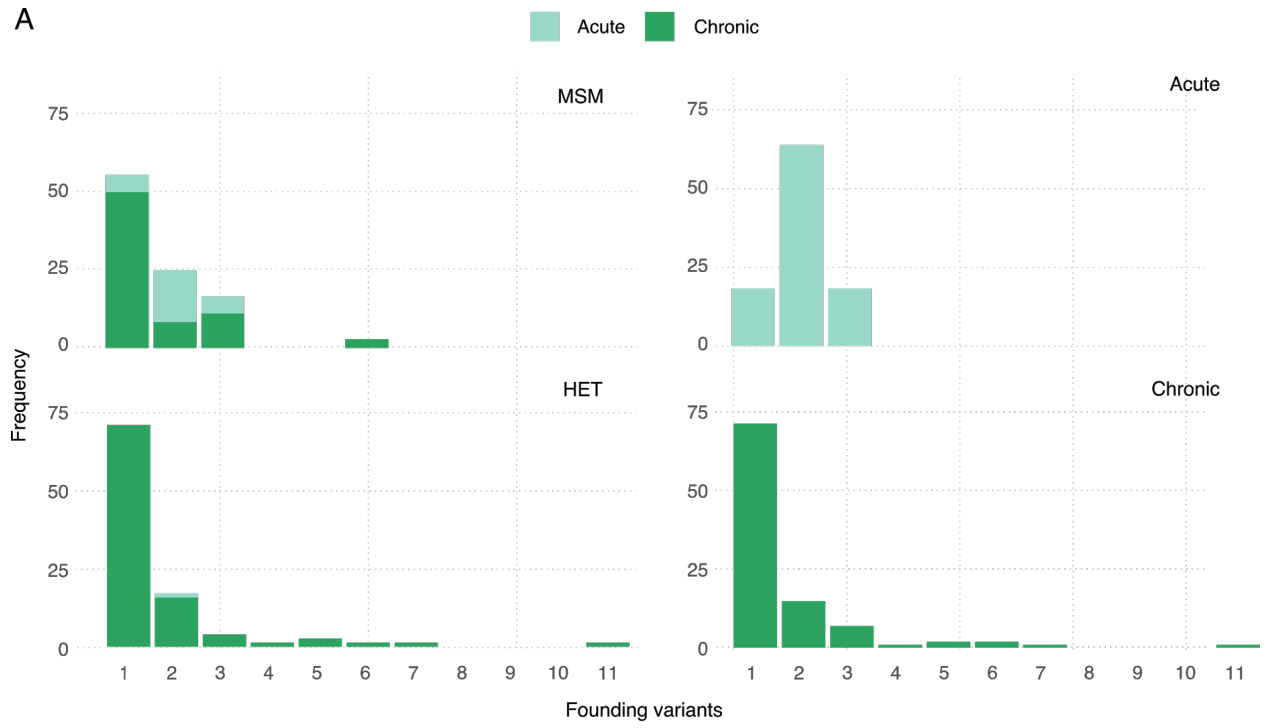
282 **inference with bootstrapping**

283 In the main analysis we used Bayesian phylogenetic reconstruction to analyse the empirical

284 sampled genetic data of each empirical transmission pair, using the respective posterior

285 distribution to calculate the frequency of each topology class (MM, PM and PP). Here we

286 provide a sensitivity analysis to calculate the tree topology class distribution of the empirical
287 sampled genetic data by maximum likelihood phylogenetic tree construction and bootstrapping.
288 After bootstrapping the empirical data 100 times to calculate the frequency of MM, PM and PP
289 topology classes for each transmission pair, we then proceeded using the same methodology as
290 in the main text. That is, we fit the simulation model (parameterised with the pair-specific data)
291 to the bootstrapped data individually for each transmission pair by comparing the frequencies of
292 tree topology classes. Overall our results remained consistent with our main results, albeit with
293 slightly lower probabilities of observing one founder variant. The median number of founder
294 variants transmitted across all pairs is 1 (range: 1-11, **Fig. S5A**). Across all pairs in both risk
295 groups, the mean probability of observing one founder variant is 0.62. Stratifying by risk group,
296 we find there is a higher probability that one variant founds HET infections than MSM infections
297 (a geometric mean of 0.67 vs. 0.53, **Fig. S5B**). Stratifying by infection stage of the source
298 partner, we find there is a much lower probability of one founder variant during the acute stage
299 than during the chronic stage (means of 0.31 vs. 0.66) with approximately twice the chance of
300 multiple founder variant transmission during acute stage infection across both risk groups
301 (relative risk is 0.47).



303 **Fig. S5: Phylogenetic findings from the calibrated simulations with bootstrapped empirical data.** A)
304 Frequency of the number of founding variants for transmission pairs by infection stage of source partner at
305 transmission and risk group. The **number of transmitted founding variants** is calculated as the modal
306 simulated value. B) Probability of one founder variant in the recipient for each pair stratified by infection
307 stage of the source partner at transmission.

308 **Effect of the number of sequences for each transmission pair**

309 Here we provide sensitivity analysis to the estimation of the probability that a single founder
310 variant was transmitted to the respective recipient by the number of sequences available from the
311 source and recipient, which ranges from 5 to 149 across all partners. First, the number of
312 sequences available from the transmitter and the recipient is correlated (*Pearson's* product-
313 moment correlation=0.53, $P<0.01$). However, we do not find any evidence of correlation
314 between the total number of sequences for a pair and the estimated number of founder variants in
315 the recipient ($P>0.2$). While an MM topology is more frequently observed when the total number
316 of sequences was small ($P<0.01$), removing the pairs with a likely MM topology do not change
317 our main result: the probability that a single founder variant was transmitted to the respective
318 recipient is lower for the acute pairs (0.402) than for the chronic ones (0.749).

319 **Effect of the sequencing method**

320 We evaluated if our results were affected by the type of sequence data used in the analysis. All of
321 the transmission pair data were generated using Sanger capillary sequencing except for those in
322 one study ((46) in **Data S1**) which used Illumina sequencing on end-point diluted primary
323 isolates. Our results are robust to the exclusion of the eight transmission pairs extracted from this

324 study: that is, the probability that a single founder variant is transmitted to the respective
325 recipient is lower for the acute stage (0.402) than for the chronic stage (0.756).

326 **Effect of the gene region and length**

327 Looking at chronic stage transmissions only, if we compare the number of founder variants
328 inferred from envelope gene sequences to those inferred from non-envelope sequences, we don't
329 find significant differences ($P>0.4$) in the probability that a single founder variant is transmitted
330 to the respective recipient: 0.739 for envelope sequences and 0.856 for non-envelope ones.

331 Conversely, if we include data from both chronic and acute transmissions, and restrict our
332 analysis to those pairs with sequences from the envelope region, our results remain unchanged.

333 That is, the probability that a single founder variant is transmitted to the respective recipient is
334 lower during the acute stage (0.432) than during the chronic stage (0.739). Finally, if we
335 condition our analysis on those pairs for whom full or near full genomes are available (17 pairs),
336 our results remain consistent with the main analysis: the probability that a single founder variant
337 was transmitted is lower for acute stage transmissions (0.138, $n=1$) than for chronic stage
338 transmissions (0.903, $n=16$). We found that length of the sequenced region is not correlated with
339 the probability that a single founder variant is transmitted to the recipient (*Pearson's* product-
340 moment correlation=0.14, $P>0.14$). Moreover, there are no significant differences ($P>0.81$) in
341 the length of the sequenced region when stratifying our data by infection stage of the source
342 partner at transmission. Together these observations indicate that our results are not influenced
343 by the length of sequenced regions.

344

345

346 **Data S1 (Separate file):** SITable_EpiGeneticData.csv. Collated epidemiological and clinical
347 data and genetic metadata for the 112 transmission pairs used in the analysis.

348 **Data S2 (Separate file):** SITable_AnalysisData.csv. Analysis information for the 112
349 transmission pairs used in the analysis.

350 **Data S3 (Separate file):** SITable_ColumnNamesKey.csv. Additional information on column
351 headers in Data S1,S2 tables

352 **Data S4 (Separate file):** Alignments.zip. Individual files of sequence alignments used in the
353 analysis for the 112 transmission pairs.

354